rice2024 Proceedings of the Ninth International Conference on Research in Intelligent Computing in Engineering pp. 147–150
DOI: 10.15439/2024R58
ISSN 2300-5963 ACSIS, Vol. 42

# Enhancing MRI Imaging Efficiency: A Hybrid Under-Sampling Strategy for k-Space Data Acquisition

Duc-Tan Tran*
Faculty of Electrical and Electronic Engineering Phenikaa University
Ha Noi, Viet Nam
tan.tranduc@phenikaa-uni.edu.vn

Quang Huy Pham,
Thi Phuong Hanh Nguyen
Electric Power University
Ha Noi, Viet Nam
{huypq, hanhntp}@epu.edu.vn

Trinh Thi Thu Huong
Hanoi University of Industry
Ha Noi, Viet Nam
huongttt@haui.edu.vn

***Abstract*—Compressed Sensing (CS) offers a promising solution to reduce MRI acquisition times, addressing challenges of prolonged scans and patient discomfort. This paper presents a new method for compressing and reconstructing MRI images using k-space gradients. A hybrid under-sampling approach allocates 80% of measurements to random sampling and 20% to deterministic sampling near the k-space center. Additionally, it explores the impact of reducing kx samples by 15%, 25%, and 50% on image quality. Reconstruction uses a nonlinear conjugate gradient method, with image quality assessed via a similarity index Q. Results show the proposed CS approach effectively compresses MRI data while preserving essential image quality, optimizing protocols and reducing scan times.**

***Index Terms*—Compressed Sensing (CS), MRI reconstruction, Nonlinear conjugate gradient descent, Image quality assessment, Frequency domain (k-space)**

## I. Introduction

THERE are a lot of researches that explore advanced techniques in MRI to enhance imaging speed, resolution, and diagnostic accuracy. Larkman and Nunes [1] provide a comprehensive review of parallel MRI techniques, which significantly reduce scan times by simultaneously acquiring multiple lines of k-space. Griswold et al. [2] introduce the GRAPPA method, a powerful parallel imaging technique that improves image quality without increasing acquisition time. Kazmierczak et al. [3] and Yoon et al. [4] demonstrate improved lesion detection and arterial phase imaging using innovative MRI sequences like CAIPIRINHA and triple arterial phase techniques, respectively. Hope et al. [5] focus on optimizing gadoxetate-enhanced imaging with high spatio-temporal resolution sequences to capture arterial phases more effectively.

Compressed Sensing (CS) has emerged as a promising approach in medical imaging, particularly in MRI, where it enables efficient image acquisition by reconstructing high-quality images from a reduced number of samples. The need for accelerated imaging techniques is driven by the desire to decrease scanning times, reduce patient discomfort, and improve workflow in clinical environments. CS exploits the sparsity of image data in a transform domain, allowing significant reductions in data acquisition without compromising image quality [6-11].

The objective of this work is to demonstrate the efficacy of CS in MRI data compression and reconstruction, providing a foundation for further research into advanced CS algorithms that could optimize MRI acquisition protocols [12-18]. In this study, we applied 80% of the measurements to random under-sampling and 20% to deterministic under-sampling near the center of k-space to MR imaging. A fixed compression ratio of 0.2 was used to retain only 20% of the original image data, reflecting a realistic compression scenario. Although kx data is typically acquired quickly in a single shot per TR, the impact of reducing kx samples by 15%, 25%, and 50% on image quality is also explored. The transformation of MRI data into k-space and subsequent reconstruction using a nonlinear conjugate gradient descent approach were critical steps in this process. The quality of the reconstructed images was quantitatively assessed by calculating a quality index Q, which considers the mean intensity, variance, and covariance between the original and reconstructed images. This index enables a detailed evaluation of the effectiveness of CS in maintaining image fidelity and highlights the potential of CS for improving MRI efficiency in medical diagnostics.

## II. Method

m(x, y) is assumed to be a MRI image. To obtain m(x, y) using the 2D-Fourier transform:

$$v\left(k_x, k_y\right) = \sum_{n_x}^{N_x-1} \sum_{n_y}^{N_y-1} m\left(n_x, n_y\right) e^{-i\left(k_x x + k_y y\right)} \quad (1)$$

where Nx and Ny are in x and y axes. We uses the Cartesian trajectory for 2D imaging, and the power-law follows the encoded information density of the k-space.

A high degree of sparsity is required for MR images since it implies that a small amount of information can convey the substance of the data. The sparsity of these images can be represented using a variety of transform techniques, including DWT, DCT, and FFT. Only 2D Cartesian sampling is the subject of this investigation. It has been discovered that the artifacts will appear as coherent replicas of the image structure when standard Cartesian under-sampling is used.

*—Corresponding author

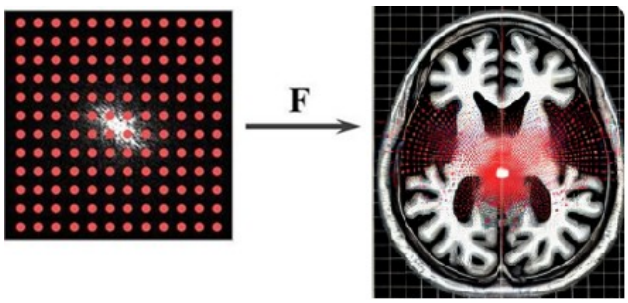


Fig. 1 Transformation between the k-space domain and the magnetic resonance image

Fourier basis functions' low-frequency components are located in k-space's origin. Thus, by collecting encoded information surrounding the origin of k-space, we can improve the performance of MR image reconstruction.

For a given value of the under-sampling ratio r ($0 < r < 1$), we divided the number of measurements in the (ky) dimension in half: Eighty percent of the measurements are for random under-sampling, while twenty percent are for specific under-sampling made at the k-space origin (see Algorithm 1).

**Algorithm 1.** Our proposed MRI measurement

*Step 1*: Set up for RF excitation
*Step 2*: Define r = M/N, and select its component $r_1$ for random sampling and $r_2$ for regular sampling such as $r = r_1 + r_2$
*Step 3*: Determine the number of $k_y$ patterns ($N_1$) and their coordinates $< k_x, k_y >$ in k-space using random sampling based on $r_1$
*Step 4* Determine the number of $k_y$ patterns ($N_2$) and their coordinates $< k_x, k_y >$ from the center of k-space to the periphery based on $r_2$
4.1 Initialize i = 1
4.2 Select one $k_y$ pattern starting from the center towards the periphery.
4.3 If the selected pattern overlaps with any pattern from the random sampling (Step 3), repeat Step 4.2.
4.4 If the pattern is unique, increment i by 1. Proceed to Step 5 if $i>N_2$
4.5 Choose $k_x$ samples in 100%, 85%, 75%, and 50% of the total number of $k_x$
4.6 Jump to 4.2

The proposed MRI measurement algorithm focuses on optimizing the sampling process in *k*-space to improve image reconstruction efficiency while reducing scan time. The algorithm begins with setting up RF excitation and defining a compression ratio r=M/N, which is split into two components: $r_1$ for random sampling and $r_2$ for regular sampling, ensuring $r=r_1+r_2$. It first employs random sampling to determine the $N_1$ patterns in k-space, based on $r_1$. Subsequently, the algorithm shifts to a regular sampling strategy to select N2 patterns starting from the center of k-space and moving towards the periphery, as dictated by $r_2$. This step includes a check to avoid overlap with previously selected random patterns, ensuring uniqueness in sampling. If a conflict is detected, the algorithm re-selects until a unique pattern is found. It then increments the count until iii exceeds $N_2$, moving to the next phase. Furthermore, for each unique $k_y$ pattern, the algorithm diversifies the sampling density along the $k_x$ axis, utilizing different proportions (100%, 85%, 75%, and 50%) of the total $k_x$ samples, thereby enhancing the flexibility in capturing critical spatial frequencies. By combining random and regular sampling techniques, the algorithm aims to optimize the information captured in k-space, thus improving the quality of compressed sensing MRI while minimizing acquisition time and computational load.

The reconstructed image is obtained by:

$$\hat{m} = \arg\min_{m} \left( \|F_u m - y\|_2^2 + \lambda \|\Psi\|_1 \right) \quad \text{subject to} \quad \|F_u m - y\|_2 < \varepsilon \tag{2}$$

where y is the measured value, Ψ is the operator for the sparsifying transform, and Fu is the Fourier operator. The error between the recovered object and the original object is

$$\varepsilon = \frac{1}{N \times M} \sum_{i=1}^{N} \sum_{j=1}^{M} |m_{ij} - \hat{m}_{ij}| \tag{3}$$

The universal image quality index (Q), another performance metric, is also employed

$$Q = \frac{4 \sigma_{xy} . \bar{x} . \bar{y}}{(\sigma_x^2 + \sigma_y^2)[(\bar{x})^2 + (\bar{y})^2]} \tag{4}$$

When two images are identical, the Q index hits 1.

## III. Results and Discussion

In order to demonstrate the benefit of the suggested approach, the ε from reconstructed images is first evaluated using a compression ratio of 0.2. In the ky dimension, we study a hybrid under-sampling strategy, distributing 20% of the measurements to deterministic under-sampling close to the center of k-space and 80% of the measurements to random under-sampling. As seen in Fig. 2, the original brain MR slice with an image size of 128 × 128 served as the data source for the numerical simulation. This method offers a structured approach for testing and assessing compressed

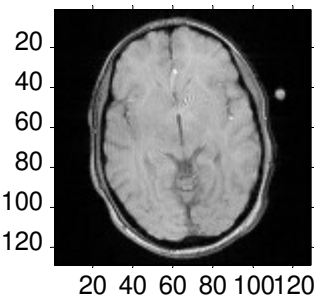


Fig. 2 The original brain MR slice image.

sensing techniques in MRI, enabling comparison of various reconstruction techniques and evaluation of their quality.

Fig. 3 shows the effect of different levels of k-space sampling on MRI image reconstruction quality. In each row, a binary mask (left column) represents the sampling pattern used in k-space, with white lines indicating sampled points and black areas representing unsampled points. The percentages (100%, 85%, 75%, and 50%) refer to the sampling density in kx, with 100% representing full sampling and the lower percentages corresponding to increasing levels of under-sampling. As the sampling density decreases, the MRI images (right column) progressively lose detail, displaying more noise and artifacts. At 100% sampling, the image is clear and well-defined. At 85% and 75% sampling, the images still retain relatively good quality but begin to show slight blurring. However, at 50% sampling, the image quality significantly deteriorates, with more noticeable blurring and loss of detail. This visual comparison illustrates how under-sampling in k-space affects image quality, demonstrating the trade-off between acquisition speed and image fidelity in MRI.

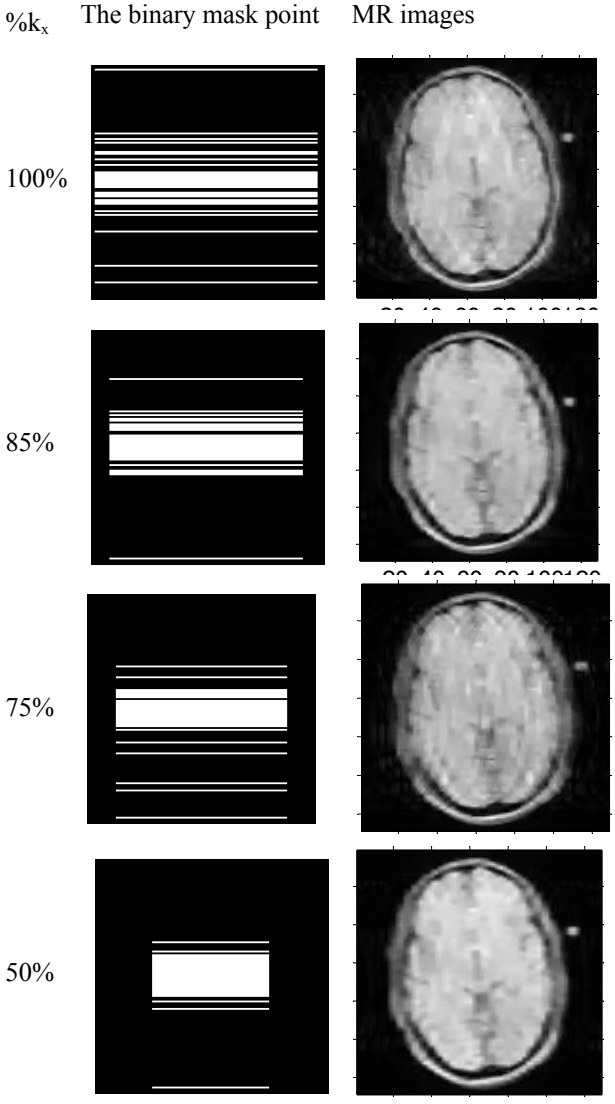


Fig. *3* Reconstructed brain MR slice images

Table 1 presents the performance parameters of MRI image reconstruction under different k-space sampling densities (%kx). The table provides two key metrics: Error and Q index, which evaluate the quality of the reconstructed images. The results in Table 1 demonstrate a clear trade-off between the MRI scan time (which decreases with lower sampling densities) and the image quality (which decreases with higher Error and lower Q index). At 50% sampling, while the scan time would be significantly reduced, the increased Error and lower Q index indicate a noticeable drop in image clarity, which may not be suitable for diagnostic purposes. On the other hand, the performance at 75% and 85% sampling densities shows a promising compromise, where the reduction in scan time does not drastically affect the image quality. This could be particularly useful in clinical settings where reducing patient discomfort and motion artifacts is crucial.

TABLE 1. PERFORMANCE PARAMETERS

| $\%k_x$ | Error | Q index |
|---|---|---|
| 100% | 525.8777 | 0.9721 |
| 85% | 592.2455 | 0.9681 |
| 75% | 503.2018 | 0.9674 |
| 50% | 854.2210 | 0.9487 |

## IV. CONCLUSION

This study demonstrates the effectiveness of Compressed Sensing (CS) in reducing MRI acquisition requirements while preserving essential image quality. By applying 80% of the measurements to random under-sampling and 20% to deterministic under-sampling near the center of k-space, we generated compressed representations of MRI data in the frequency (k-space) domain, which were then reconstructed using a nonlinear conjugate gradient descent approach. The quality assessment, based on a calculated error and quality index Q, indicating that CS can retain key image details even at significant compression levels.

The results underscore the potential of CS techniques to optimize MRI protocols, offering a path to shorter scan times and enhanced patient comfort without compromising diagnostic accuracy. Future work could explore the application of more advanced CS algorithms, potentially improving reconstruction quality further and expanding the clinical viability of CS in MRI.

## REFERENCES

[1] D. J. Larkman, R. G. Nunes, Parallel magnetic resonance imaging, Phys. Med. Biol., 52 (2007), R15−R55.
[2] M. A. Griswold, P. M. Jakob, R. M. Heidemann, M. Nittka, V. Jellus, J. Wang, et al., Generalized autocalibrating partially parallel acquisitions (GRAPPA), Magnet. Reson. Med., 47 (2002), 1202−1210.
[3] P. Kazmierczak, D. Theisen, K. Thierfelder, W. Sommer, M. Reiser, M. Notohamiprodjo, et al., Improved detection of hypervascular liver lesions with CAIPIRINHA-Dixon-TWIST-volume-interpolated breath-hold examination, Invest. Radiol., 50 (2014), 153−160.
[4] J. H. Yoon, J. M. Lee, M. H. Yu, E. J. Kim, J. K. Han, Triple arterial phase MR imaging with gadoxetic acid using a combination of contrast

enhanced time robust angiography, keyhole, and viewsharing techniques and two-dimensional parallel imaging in comparison with conventional single arterial phase, Korean .J. Radiol., 4 (2016), 522−532.

[5] T. A. Hope, M. Saranathan, I. Petkovska, B. A. Hargreaves, R. J. Herfkens, S. S. Vasanawala, Improvement of gadoxetate arterial phase capture with a high spatio-temporal resolution multiphase three-dimensional SPGR-Dixon sequence, J. Magn. Reson. Imaging, 38 (2013), 938−945.

[6] D. L. Donoho, Compressed sensing, IEEE Trans. Inf. Theory, 52 (2006), 1289−1306.

[7] F. Ong, R. Heckel, K. Ramchandran, A Fast and Robust Paradigm for Fourier Compressed Sensing Based on Coded Sampling, in ICASSP 2019−2019 IEEE International Conference on Acoustics, Speech and Signal Processing (ICASSP), 2019.

[8] Y. Li, R. Yang, Z. Zhang, Y. Wu, Chaotic-like k-space trajectory for compressed sensing MRI, J. Med. Imaging. Health. Inform., 5 (2015), 415−421.

[9] T. Tran Duc, P. Dinh Van, C. Truong Minh, L. T. Nguyen, Accelerated Parallel Magnetic Resonance Imaging with Multi-Channel Chaotic Compressed Ssensing, in The 2010 International Conference on Advanced Technologies for Communications, 2010.

[10] M. Lustig, D. Donoho, J. M. Pauly, Sparse MRI: The application of compressed sensing for rapid MR imaging, Magnet. Reson. Med., 58 (2007), 1182−1195.

[11] G. Wang, Y. Bresler, V. Ntziachristos, Guest editorial compressive sensing for biomedical imaging, IEEE Trans. Med. Imaging, 30 (2011), 1013−1016.

[12] J. A. Tropp, A. C. Gilbert, Signal recovery from random measurements Vvia orthogonal matching pursuit, IEEE Trans. Inf. Theory, 53 (2007), 4655−4666.

[13] E. J. Candes, J. Romberg, T. Tao, Robust uncertainty principles: Exact signal reconstruction from highly incomplete frequency information, IEEE Trans. Inf. Theory, 52 (2006), 489−509.

[14] K. H. Jin, D. Lee, J. C. Ye, A general Fframework for compressed sensing and parallel MRI Uusing a filter based low-rank hankel matrix, IEEE Trans. Comput. Imaging, 2 (2016), 480−495.

[15] G. Yang, S. Yu, H. Dong, G. Slabaugh, P. L. Dragotti, X. Ye, et al., DAGAN: Deep De-aliasing generative adversarial networks for fast compressed sensing MRI reconstruction, IEEE Trans. Med. Imaging, 37 (2018), 1310−1321.

[16] K. Thurnhofer-Hemsi, E. López-Rubio, E. Domínguez, R. M. Luque-Baena, N. Roé-Vellvé, Deep learning-based super-resolution of 3D magnetic resonance images by regularly spaced shifting, Neurocomputing, 398 (2020), 314−327.

[17] Tran, A. Q., Nguyen, T. A., Duong, V. T., Tran, Q. H., Tran, D. N., & Tran, D. T. (2020). MRI Simulation-based evaluation of an efficient under-sampling approach. Mathematical Biosciences and Engineering, 17(4), 4048-4063.

[18] Tran, A. Q., Nguyen, T. A., Doan, P. T., Tran, D. N., & Tran, D. T. (2021). Parallel magnetic resonance imaging acceleration with a hybrid sensing approach. Mathematical Biosciences and Engineering, 18(3), 2288-2302.